Reduction of Output Common Mode Voltage using a Novel SVM Implementation in Matrix Converters for Improved Motor Lifetime

Jordi Espina, Carlos Ortega, *Member*, *IEEE*, Liliana de Lillo, *Member*, *IEEE*, Lee Empringham, *Member*, *IEEE*, Josep Balcells, *Senior Member*, *IEEE*, Antoni Arias, *Member*, *IEEE*.

Abstract— **This paper presents the study of an alternative Space Vector Modulation (SVM) implementation for Matrix Converters (MC) which reduces the output Common Mode (CM) voltage. The strategy is based on replacing the MC zero vectors by the rotating ones. In doing this, the CM voltage can be reduced which in-turn reduces the CM leakage current. By reducing the CM current, which flows inside the motor through the bearings and windings, the Induction Motor (IM) deterioration can be slowed down. The paper describes the SVM pattern and analyses the CM voltage and the leakage current paths. Simulation and experimental results based on a MC-IM drive are provided to corroborate the presented approach.**

Index Terms— **Matrix converter, space vector modulation, common mode voltage, leakage currents, bearing degradation.**

I. INTRODUCTION

Thanks to the rapid development of power electronic devices, modern power electronic converters (PEC) have undergone a continuous evolution since they emerged. This has permitted the high performance and accurate control of electrical machines. However, Common Mode Voltage (CMV) produced by modern PECs is known to be one of the main sources of early motor winding failure and bearing deterioration. High frequency components and large amplitudes of the CMV at the motor neutral point have been shown to generate high frequency currents to the ground path and induce voltages on the rotating shaft[1], which eventually reduces the machine operational life [2-6].

There are a wide number of scientific papers that have studied the effects of leakage currents inside electrical motors [4, 5, 7-12]. Two of the main consequences are damage to the isolation material of the windings and destruction of the

J. Espina, L. Empringham and L. de Lillo are with Power Electronic Machines and Control group at the University of Nottingham, Nottingham, NG7 2RD, U.K.

J. Balcells and A. Arias are with the Electronics Engineering Department, Universitat Politècnica de Catalunya, 08034 Barcelona, Spain.

C. Ortega is with the Electronics Engineering Department, Escola Universitària Salesiana de Sarrià, 08017 Barcelona, Spain (e-mail: cortega@euss.es).

bearings. In [7, 8, 13-15] a large study of the leakage current phenomena and its consequences is presented. This study defines four types of leakage currents that are produced by different CMV effects. Two of them are very harmful for the bearings, where they create flutings on the rolling path and deteriorate the lubricant. Essentially, these two currents create voltages known as bearing voltage v_b and shaft voltage v_{sh}, which are the mirror of the CMV. Bearing voltage is created via a parasitic capacitance voltage divider and the shaft voltage is induced via an electromagnetic flux (as in a transformer), where this flux is produced by winding-to-frame HF current [13].

Several methods to reduce the CMV have been proposed in the literature [1, 11, 16, 17], however, these methods seem to be limited to three-phase Pulse Width Modulation (PWM) rectifier-inverter systems.

Recently other PEC topologies have received considerable attention and can be seen as a good potential alternative to the standard VSI for some applications. During the last decade, special attention has been paid to Matrix Converters (MC) due to its relevant advantages such as controllable input power factor and a very compact design [18-24].

Some strategies to reduce the CMV using direct MC have been adapted from the ones using VSI and others have arisen from new contributions using the advantages of MC. One of the most popular techniques to reduce CMV is to use the correct zero vector, from the three the MC can create, which introduces the smallest amplitude to all output phases [25]. Another technique is based on the use of a two opposite active vectors, with the smallest amplitude, instead of zero vectors [26]. A similar strategy, but applied in direct torque control, was presented in [27]. A predictive strategy, which tries to forecast, at every sampling period, which vector is the best option, has been presented in [28]. This strategy uses a Quality Function Minimization (QFM) which has to consider different parameters such as, output voltage, input power factor and CMV. This contribution is based on the use of all available vectors including the rotating ones. Hardware modifications such as a three phase open-end-winding AC machine driven by two direct MC is presented in [29]. This topology uses only rotating vectors to control the ac machine, which completely avoids the CMV and claims to increase by up to 150% the operating region at constant torque. CMV reduction in indirect
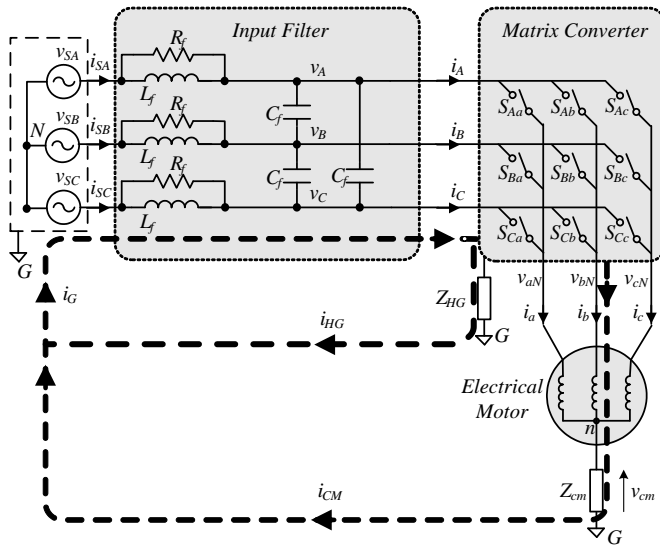
Fig. 1. Matrix Converter scheme and leakage path.

MC is discussed in [30, 31].

This paper presents a study of the modulation strategy introduced in [32], In [32] a brief introduction of using rotating vectors was presented. This paper expands and analyses the method including both simulation and experimental validation. The modulation technique consists of the replacement of the zero vectors used in doubled-sided space vector modulation (DSSVM) by the rotating vectors [33]. The rotating vectors applied within DSSVM pattern reduces the CM voltage amplitude which is the source of the CM leakage currents and hence, increasing the motor lifetime. An extensive comparison between standard DSSVM and the modulation strategy is presented in this paper. Simulation and experimental results of both methods corroborating the CMV reduction are also shown.

II. MATRIX CONVERTER

The MC is an advanced AC-AC circuit topology enabling the generation of load voltage with arbitrary amplitude and frequency, bi-directional power flow, sinusoidal input/output waveforms, and operation with unity input displacement factor [24, 34-36]. Since no intermediate reactive devices are required, a MC allows for a very compact design. In addition to these advantages, its low cost and high power density have made MC an attractive solution for special applications such as compact drives, drives in hostile environments, military applications [37], aerospace [38], and renewable energy [39-41].

However, the MC has some potential drawbacks, more complex control, a higher number of power switches and limited ride through capability [42]. All these drawbacks are being addressed as the technology becomes more mature making this converter topology a hot topic of research [21, 43].

Although many different structures have been proposed in the literature [34], from a practical point of view, the three-phase, 3x3 switch MC shown in Fig. 1 is the most widely researched as it connects a three-phase load into a three-phase

TABLE I
MC OUTPUT VOLTAGE & INPUT CURRENT VECTORS

	$a\ b\ c$	$|\vec{v}_o|$	α_o	$|\vec{i}_i|$	β_i
+1	$A\ B\ B$	$2/3v_{AB}$	0	$2/\sqrt{3}\ i_a$	$11\pi/6$
+2	$B\ C\ C$	$2/3v_{BC}$	0	$2/\sqrt{3}\ i_a$	$\pi/2$
+3	$C\ A\ A$	$2/3v_{CA}$	0	$2/\sqrt{3}\ i_a$	$7\pi/6$
+4	$B\ A\ B$	$2/3v_{AB}$	$2\pi/3$	$2/\sqrt{3}\ i_b$	$11\pi/6$
+5	$C\ B\ C$	$2/3v_{BC}$	$2\pi/3$	$2/\sqrt{3}\ i_b$	$\pi/2$
+6	$A\ C\ A$	$2/3v_{CA}$	$2\pi/3$	$2/\sqrt{3}\ i_b$	$7\pi/6$
+7	$B\ B\ A$	$2/3v_{AB}$	$4\pi/3$	$2/\sqrt{3}\ i_c$	$11\pi/6$
+8	$C\ C\ B$	$2/3v_{BC}$	$4\pi/3$	$2/\sqrt{3}\ i_c$	$\pi/2$
+9	$A\ A\ C$	$2/3v_{CA}$	$4\pi/3$	$2/\sqrt{3}\ i_c$	$7\pi/6$
-1	$B\ A\ A$	$-2/3v_{AB}$	0	$-2/\sqrt{3}\ i_a$	$11\pi/6$
-2	$C\ B\ B$	$-2/3v_{BC}$	0	$-2/\sqrt{3}\ i_a$	$\pi/2$
-3	$A\ C\ C$	$-2/3v_{CA}$	0	$-2/\sqrt{3}\ i_a$	$7\pi/6$
-4	$A\ B\ A$	$-2/3v_{AB}$	$2\pi/3$	$-2/\sqrt{3}\ i_b$	$11\pi/6$
-5	$B\ C\ B$	$-2/3v_{BC}$	$2\pi/3$	$-2/\sqrt{3}\ i_b$	$\pi/2$
-6	$C\ A\ C$	$-2/3v_{CA}$	$2\pi/3$	$-2/\sqrt{3}\ i_b$	$7\pi/6$
-7	$A\ A\ B$	$-2/3v_{AB}$	$4\pi/3$	$-2/\sqrt{3}\ i_c$	$11\pi/6$
-8	$B\ B\ C$	$-2/3v_{BC}$	$4\pi/3$	$-2/\sqrt{3}\ i_c$	$\pi/2$
-9	$C\ C\ A$	$-2/3v_{CA}$	$4\pi/3$	$-2/\sqrt{3}\ i_c$	$7\pi/6$
0_A	$A\ A\ A$	0	….	0	….
0_B	$B\ B\ B$	0	….	0	….
0_C	$C\ C\ C$	0	….	0	….
$+r_1$	$A\ B\ C$	v_{JMAX}	$[v_{JMAX}]$	i_{oMAX}	$[i_{oMAX}]$
$+r_2$	$C\ A\ B$	v_{JMAX}	$[v_{JMAX}+2\pi/3]$	i_{oMAX}	$[i_{oMAX}+2\pi/3]$
$+r_3$	$B\ C\ A$	v_{JMAX}	$[v_{JMAX}+4\pi/3]$	i_{oMAX}	$[i_{oMAX}+4\pi/3]$
$-r_1$	$A\ C\ B$	v_{JMAX}	$[-v_{JMAX}]$	i_{oMAX}	$[-i_{oMAX}]$
$-r_2$	$B\ A\ C$	v_{JMAX}	$[-v_{JMAX}+2\pi/3]$	i_{oMAX}	$[-i_{oMAX}+2\pi/3]$
$-r_3$	$C\ B\ A$	v_{JMAX}	$[-v_{JMAX}+4\pi/3]$	i_{oMAX}	$[-i_{oMAX}+4\pi/3]$

power supply [44]. From Fig. 1, it can be noted that the three MC phases allow any output phase to be connected to any input phase. Only two restrictions have to be considered; the input phases should never be short circuited and the output phases should never be unconnected. Therefore, just 27 switching configurations, shown in Table I, are possible.

Where, $\vec{v}_o$ is output voltage vector, $\vec{i}_i$ is input current vector, ±1-±9 are active vectors, 0_A-0_C are zero vectors and $\pm r_1$-$\pm r_3$ are rotating vectors [33],[44].

III. COMMON MODE VOLTAGE

This work is concerned with the effects produced by the current that flows through the leakage paths inside electrical machines. This leakage current is split and flows mainly through two different paths: between windings and chassis and through the bearings. These leakage paths can be enumerated as follows [2, 3, 6-8]:

1) Small capacitances between bearing's layers.
2) Electric discharge machining (EDM) paths.
3) High frequency (HF) circulating bearing currents.
4) Leakage currents due to rotor ground currents.

These currents are produced due to different effects of CMV, its amplitude and fast voltage transitions dv/dt as presented in [13]. Types 1 and 4 are HF currents that flow from windings and the motor frame to ground and through the bearings due to parasitic capacitances. These currents do not damage the bearings but creates the main CM EMI perturbations.
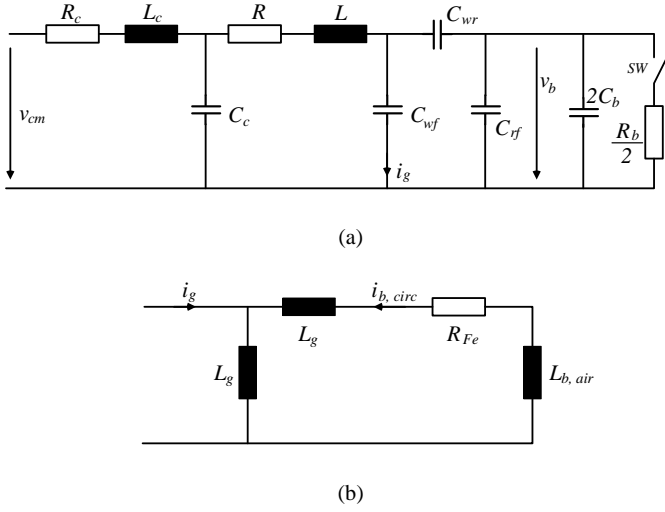
(a)

(b)

Fig. 2. (a) Simplified HF equivalent circuit of motor and cable. (b) Equivalent "transformer circuit" for calculating the current induced along the shaft.

Type 2, bearing voltage appears due to the voltage divider created between the motor's parasitic capacitances due to the winding-to-rotor, rotor-to-frame and bearing capacitances. When the electrical machine is rotating, the distance between the motor shaft and bearings is very small. This space is filled with a lubrication film. If v_b achieves the threshold voltage of the lubrication film (aprox. 5V-30 V) then a damaging EDM current pulse is produced [7]. Type 3, is a current that flows through the parasitic capacitance between stator winding to frame which induces a circular flux around the motor shaft. This flux induces voltage along the shaft (between bearings) which if it is high enough to create EDM will deteriorate the insulation properties of the lubrication oil.

Figure 2 shows equivalent circuits obtained from [15] which allow the calculation of bearing currents and voltages. Where R_c, L_c and C_c are impedance components of the motor cable; R, L are HF motor winding resistance and inductances; C_{wf} is the parasitic capacitance, winding-to-frame; C_{wr} is the parasitic capacitance, winding-to-rotor; C_{rf} is the parasitic capacitance, rotor-to-frame; C_b is the parasitic bearing capacitance and R_b is the parasitic bearing resistance. When SW is closed, this corresponds the EDM effect.

The voltage ratio between v_b and v_{cm} can estimated via (1)

$$BVR = \frac{v_b}{v_{cm}} = \frac{C_{wr}}{C_{wr} + C_{rf} + 2C_b} \tag{1}$$

The mathematic definitions of main components are defined in equations (2), (3) and (4).

$$C_{wr} = \frac{\varepsilon_0 l_{Fe} \pi d_{si}(s_Q/\tau_Q)}{\delta + h_o + h_w/3} \tag{2}$$

where ε_0 is the permittivity of air, ε_r is the relative permittivity, δ is the air gap size, l_{Fe} is the iron stack length, d_{si} is the internal diameter of stator iron stack at the air gap, s_Q is the slot opening, τ_Q is the slot pitch, h_o is the tooth tip height and h_w is the thickness of the wedge and slot insulation.

$$C_{rf} = \varepsilon_0 l_{Fe} \pi d_{si}(s_Q/\tau_Q)/(k_c \delta) \tag{3}$$

where k_c is Carter's coefficients.
The per-phase winding-frame capacitance is defined in (4)

$$C_{wf,ph} = \varepsilon_{r,eq} \varepsilon_0 l_{Fe}(Q/3) \cdot U_{slot}/(d_{slot}/F_c) \sim h^2 \tag{4}$$

where d_{slot} is the slot insulation thickness, U_{slot} is the slot circumference, h is the frame size, Q is number of stator slots and F_c is the round wire factor in the slots.

The bearing capacitance is similar to the winding-rotor capacitance, $C_b \approx C_{wr}$. The internal bearing resistance R_b is due to the discharge channel created through the lubrication film.

Figure 2.b shows the "transformer equivalent circuit" which is used to determine the circulating bearing current and induces the voltage along the shaft v_{sh}. In equation (5) describes the relation between i_g and circulating bearing current i_b.

$$\left| \frac{i_{b,circ,pk}}{i_{g,pk}} \right| = \frac{1}{2\sqrt{(1 + L_{b,air}/(2L_g))^2 + 1}} \tag{5}$$

where $L_{b,air}$ is the inductance of the path of the HF circulating BC as it encloses the air gap and end-winding cavity and L_g is the mutual inductance where is defined in (6), μ_{Fe} is the permittivity of the iron, N_{Fe} is the number of iron sheets, d_{se} is the stator external diameter, d_E is the penetration depth in the iron and h_{slot} is the slot height.

$$L_g = \mu_{Fe} \frac{N_{Fe} d_E}{4\pi} \cdot ln\left(\frac{d_{se}}{d_{si} + 2h_{slot}}\right) \tag{6}$$

It is important to determine the voltage that appears between the motor shaft and frame v_{shaft} ($v_{shaft} \approx v_b$) since its magnitude will directly contribute to possible EDM. This voltage can be obtained from equations showed above and the common-mode voltage v_{nN} at the motor's neutral point. This voltage is defined as [26, 45]:

$$v_{nN} \approx v_{cm} = \frac{(v_{aN} + v_{bN} + v_{cN})}{3} \tag{7}$$

The v_{shaft} can also be obtained by directly measuring the voltage drop between the motor shaft and frame. Moreover, some studies are focused on obtaining mathematical expressions to determine the voltage relation. In [7, 15] a mathematical model giving the relationship between v_{cm} and v_b is presented. In [8] a wide study of v_{sh} is presented, showing the transformer effect that is produced inside the motor.

Fig. 1 shows the v_{nN} and the leakage path. Where, Z_{cm} is the parasitic complex impedance which it is mainly formed by a capacitance. Although this path is the main path in which the HF current flows, it is part of the circuit that contributes to the v_b model circuit.
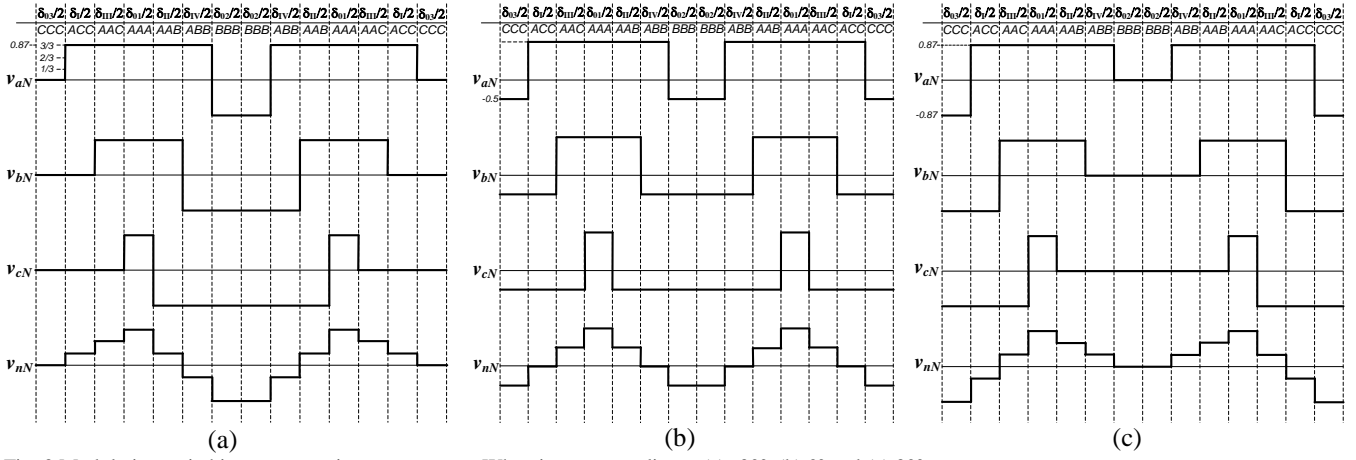.

(a)   (b)   (c)

Fig. 3 Modulation switching pattern using zero vectors. When input vector lies at (a) -30º, (b) 0º and (c) 30º.
(δ_I, δ_{II}, δ_{III}, δ_{IV}, δ_{01}, δ_{02}, δ_{03} are the SVM duty-cycles).

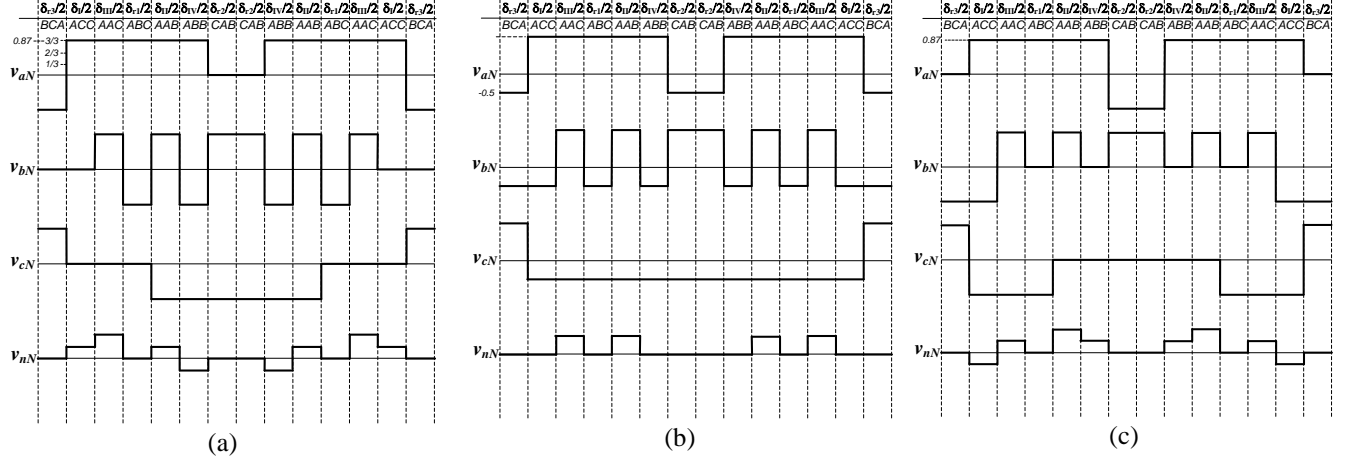(a)   (b)   (c)

Fig. 4 Modulation switching pattern using rotating vectors. When the input voltage vector lies at (a) -30º, (b) 0º and (c) 30º.
(δ_{r1}, δ_{r2}, δ_{r3} are the rotating vectors duty-cycles).
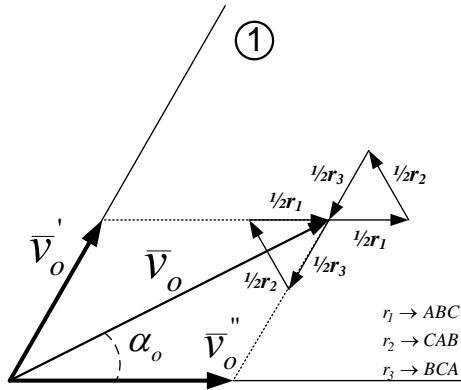
Fig. 5 Output voltage vector composition with rotating vectors.

IV. COMMON MODE REDUCTION MODULATION PATTERN

The rotating vectors are not normally used in modulation strategies as they lay in a different position at any one time, so it is difficult to create a repetitive pattern. However their contribution to the common mode voltage is null, provided that the input voltages are balanced.

Figure 3 shows the line-to-neutral voltages and the resulting CM voltage. There are three subfigures showing three important angles for sector 1, the two edges (±30º) and center (0º). The main voltage created by MC using a standard DSSVM with zero vectors is shown. Where, the reference output voltage vector is in sector 1 and the input voltage vector phase is shown at -30º, 0º and 30º inside of sector 1.

Figure 4 shows the DSSVM modulation pattern proposed when using the rotating vectors instead of the zero vectors.

Either the three positive or negative rotating vectors must be used in each pattern in order to keep the fundamental voltage unaltered as shown in Fig. 5. As an example, if +r1 is selected at the beginning of the period, then +r2 and +r3 must also be selected and used during the remainder of the sequence. The rotating vectors +r1, +r2 and +r3 replace the zero on the standard DSSVM pattern. The same duty cycles

obtained for the three nulls vectors will be applied for the three rotating ones

It can be seen in Fig. 4 that the common mode voltage v_{nN} is equal to zero whenever the rotating vectors are applied.

Fig. 5 shows the composition of the output voltage when using rotating vectors. In this particular case the output voltage vector is inside of sector 1.

The position of the rotating vectors are time varying, however, if the input voltages are balanced their contribution to both CM current and CM voltage will be zero. Equations (8) and (9) show the CM voltage and CM current contribution of the rotating vectors.

$$v_{aN} + v_{bN} + v_{cN} = 0 \tag{8}$$

$$i_a + i_b + i_c = 0 \tag{9}$$

The main improvement using rotating vectors is the 42.3% reduction of CM voltage amplitude [46]. However this modulation increases the number of commutations in each DSSVM period. In the standard DSSVM the number of commutations is 12 whereas in the modulation proposed in this paper is 16. This increment is due to the need to switch two phases when a rotating vector is selected preceded by an active one.

V. RESULTS

A comparison between the standard DSSVM using zero vectors and the proposed modulation using rotating vectors has been carried out in this section. Both, simulation and experimental tests have been carried out in order to compare the behaviour of both systems analysing, not only the CM voltage but also the THD of both the input and output currents.

Since the Matrix converter uses a capacitive input port, an inductive output load must be used and as such, an RC load was not considered. For both simulation and experimental tests, a 60 kVA MC feeding a three phase *RL* load ($R = 34\ \Omega$ and L=1.6 mH) was considered. The MC has been configured to use a modulation index of q=0.75 giving an output phase-to-neutral voltage of 120 V at 20 Hz.

A. Simulation

Figure 6 shows v_{aN}, i_a, i_{SA} and v_{nN} when the standard DSSVM is implemented.

The same voltages and currents are shown in Fig. 7 when rotating vectors are applied. As it can be observed in Fig. 7 v_{nN} peak value is approximately 100 V instead of 150 V that is reached when standard DSSVM is applied as shown in Fig. 6. Clearly v_{nN} is reduced by around 40% when rotating vectors are used.

However the rotating vectors increase the harmonic content of the input and output currents. In order to evaluate the harmonic performance when the new modulation strategy is implemented a THD study was performed, results of which are shown in Fig. 8 and 9.
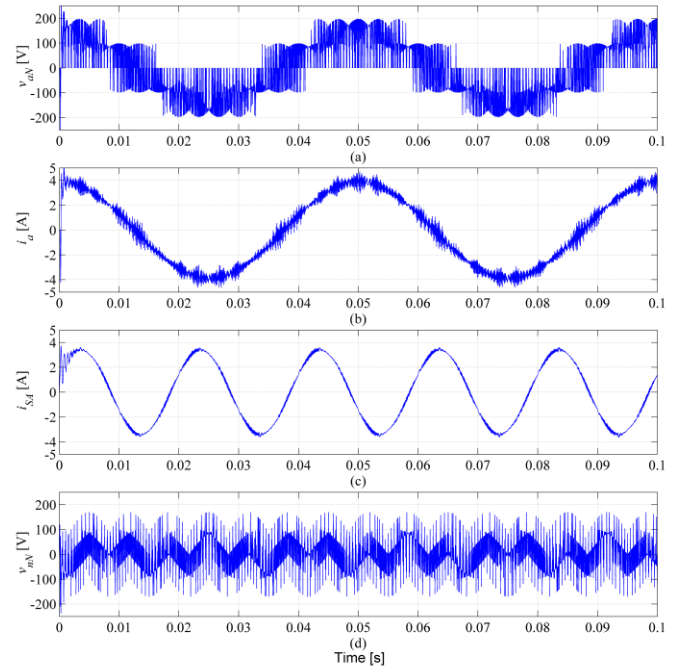

Fig. 6. Representation of voltages and currents using zero vectors. (a) output voltage phase v_{aN}. (b) output current phase i_a. (c) input current i_{SA}. (d) common voltage v_{nN}
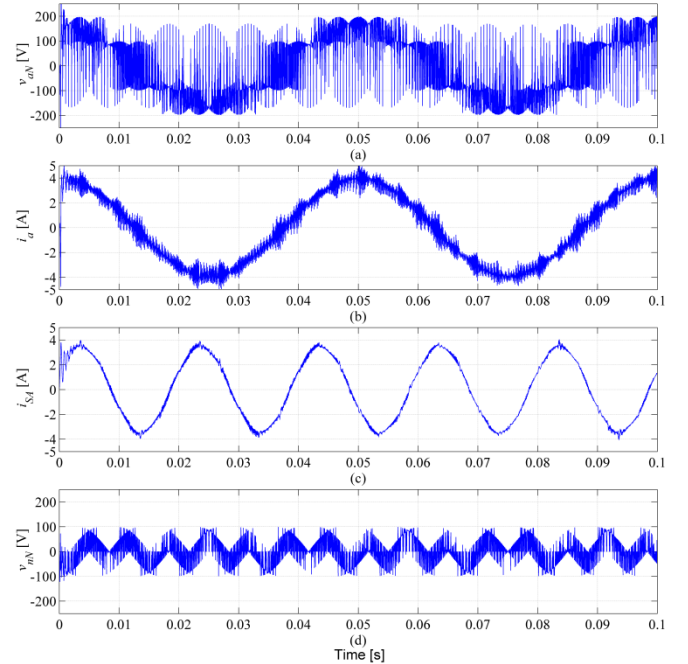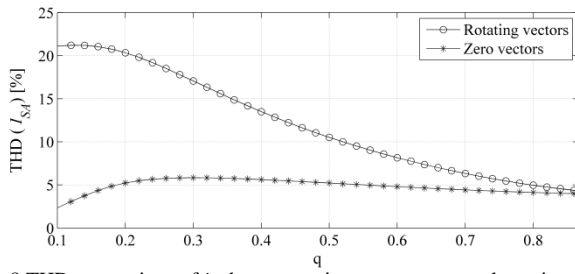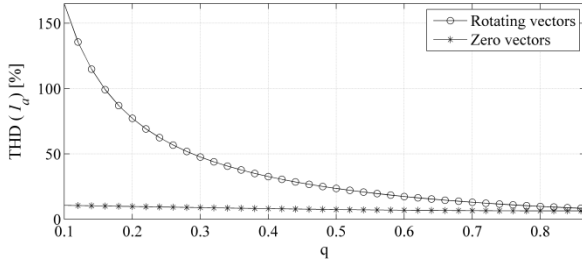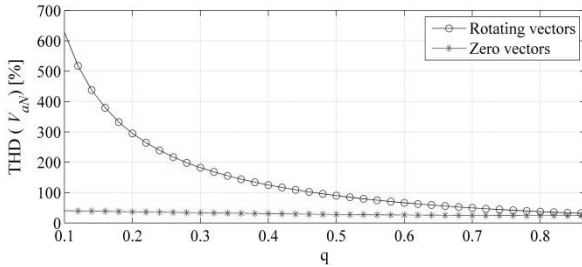

Fig. 7. Representation of voltages and currents using rotating vectors. (a) output voltage phase v_{aN}. (b) output current phase i_a. (c) input current i_{SA}. (d) common voltage v_{nN}.

Fig. 8 THD comparison of i_{SA} between using zero vectors and rotating vectors.

Fig. 9 THD comparative of i_a between using zero vectors and rotating vectors.

Fig. 10 THD comparative of v_{aN} between using zero vectors and rotating vectors.

In order to analyse and compare the harmonic content of both systems, the THD has been evaluated as a function of the modulation index. Figure 8 shows the comparison of the input current i_{SA} THD. The maximum THD produced by standard DSSVM is 6% in contrast to the 21% produced using the proposed modulation. However, when the modulation index is higher than 0.5 the THD produced by the proposed modulation is reduced considerably, from 10% with modulation index of 0.5 down to 3% with a modulation index of 0.866.

Figure 9 shows the THD comparison of the output current i_a. The THD remains constant at around 1% when the standard DSSVM is used. On the other hand, the THD using rotating vectors varies along with the modulation index. The maximum THD is around 180% when $q=0.1$ and decreases exponentially as the maximum modulation index is approached.

Figure 10 shows the evolution of the THD comparison of the output voltage when zero vectors and rotating ones are applied. This figure, as expected, corroborates the evolution of the THD output current throughout modulation index.

The THD of an induction motor load would look very similar to that shown in Fig. 9 except that the harmonic content would be reduced due to the back EMF voltage present in the motor.

It can be observed that the standard DSSVM keeps input and output current THD under moderate levels regardless of
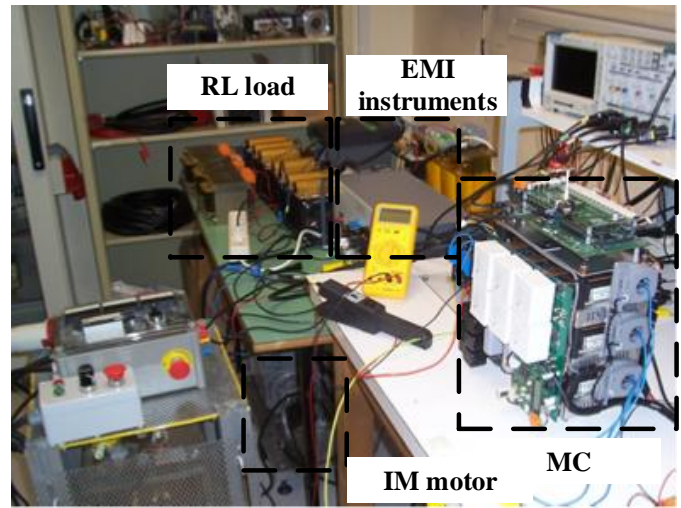

Fig. 11 Picture of experimental rig showing MC, RL load, EMI instruments and IM motor.
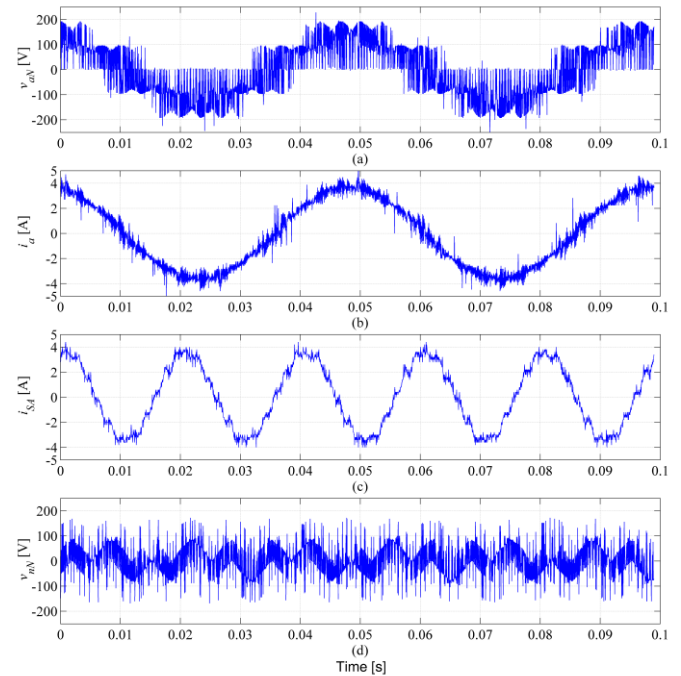

Fig. 12 Measurement using zero vectors.

the modulation index, whereas, the proposed solution introduces higher distortion at lower modulation index values. From the input and output currents THD comparison it can be concluded that the proposed modulation strategy can be suitable for modulation indexes higher than 0.5.

B. Experimental

The experimental section corroborates the simulation study which shows the important reduction on v_{nN}.

The experimental rig used to realize the comparison is composed of a direct matrix converter constructed using 200A, 1200V, common emitter connected bi-directional switches (Dynex DIM200MBS12-A000) and a three phase RL load ($R= 34\ \Omega$ and $L=1.6$ mH) connected in star configuration. This configuration has permitted the measurement of the v_{nN} voltage to compare it with simulation results. On Figure 11
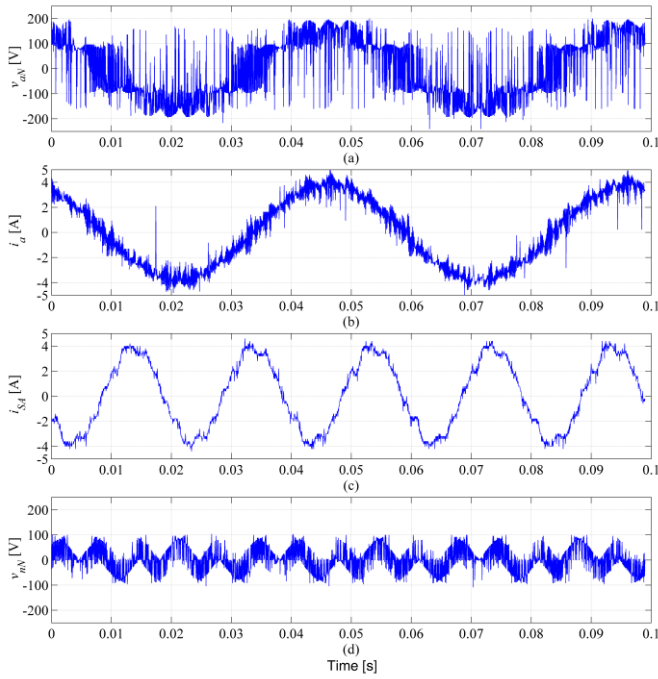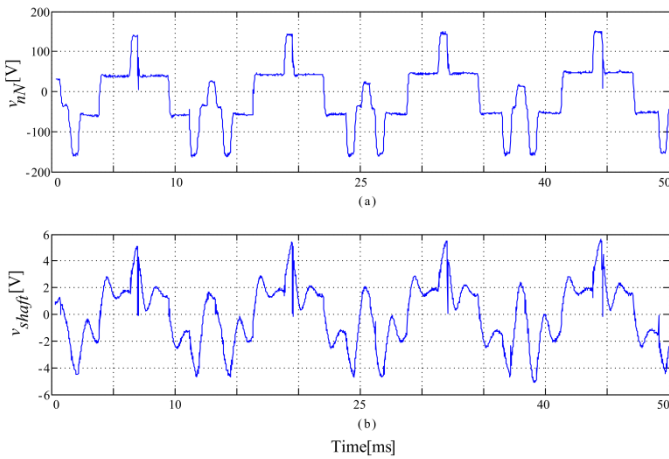
Fig. 13 Measurement using rotating vectors.

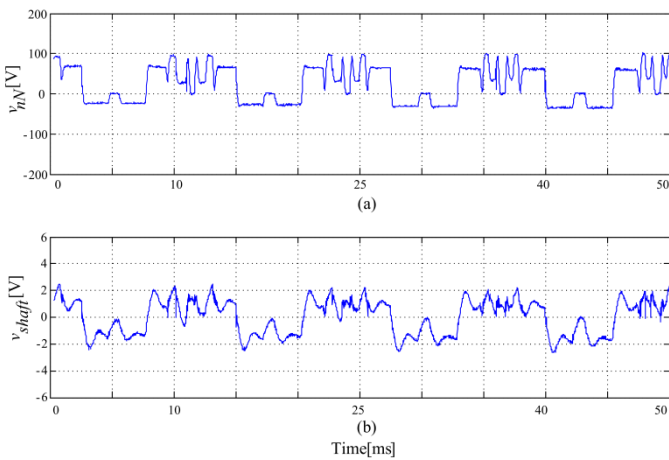Fig. 14 Voltage v_{nN} and v_{shaft} when zero vectors are applied.

Fig. 15 Voltage v_{nN} and v_{shaft} when rotating vectors are applied.
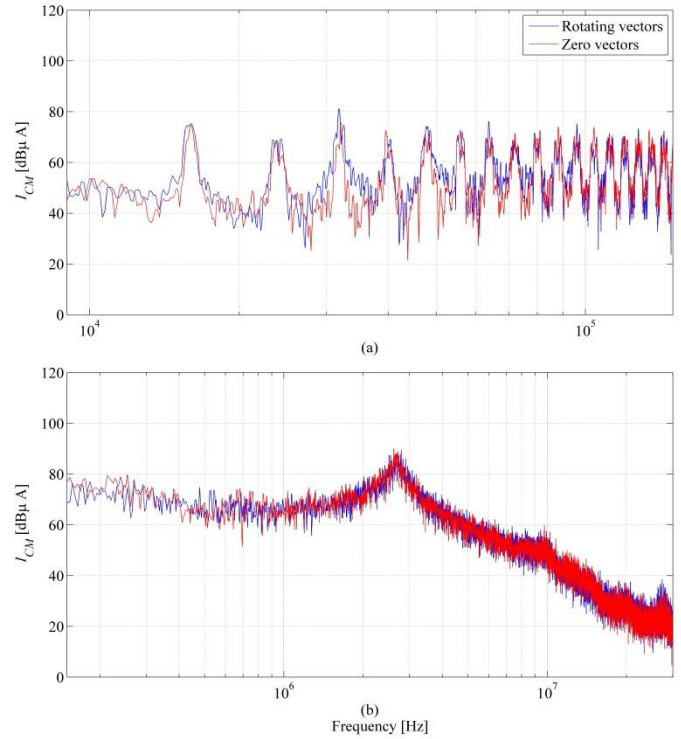
Fig. 16 Cable motor. A band and B band.

Fig. 17 Global CM current. A band, B band.
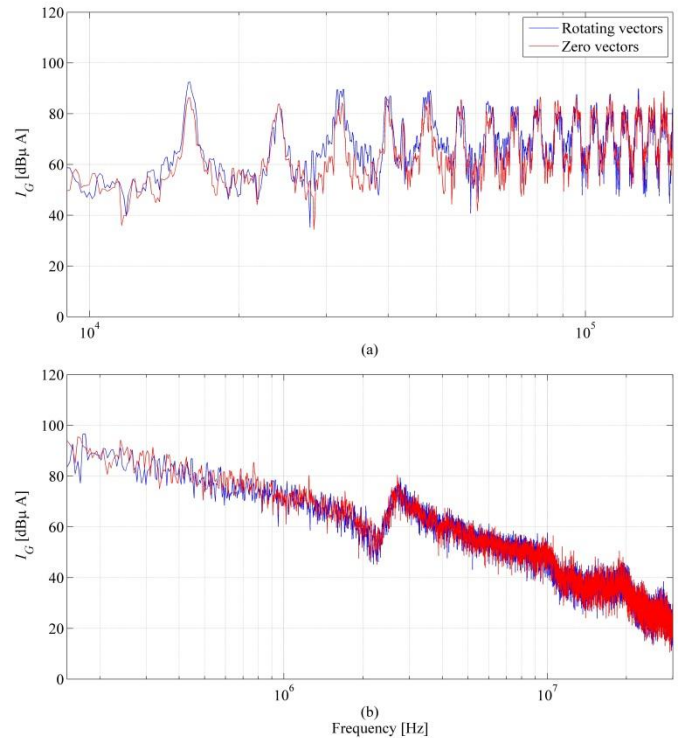
shows the experimental set-up where is shown the matrix converter and the RL load used. On the other hand, the shaft voltage v_{shaft} measurement was obtained using a 1.8 kW induction motor load connected to the MC.

As implemented in the simulation, the main variables used in the experimental rig are: $V_{AN,BN,CN} = 120$ V input voltages and q=0.75 and 20 Hz output frequency.

Figure 12 shows the main voltages and currents which describes the behaviour of MC drive when zero vectors are implemented. As it can be observed, the similarity between simulation results and experimental measurements is very high. It is fair to say that the distortion of input the current in experimental measurements is higher due to the experimental rig restrictions (dead times, protection times, measurement noise, device non-linearities, etc.).

After the validation of the simulation model with experimental tests, the DSSVM using rotating vectors has been implemented to corroborate the approach of this paper.

Figure 13 shows the experimental measurements when DSSVM using rotating vectors is applied. As shown in Fig. 13.d, v_{nN} is reduced considerably compared in Fig. 12.d, when zero vectors are used.

Other results that indicate that this modulation method extends the motor's life is shown in Fig. 14 and 15. These figures show the voltage measurement between the motor shaft and frame when zero vectors and rotating vectors are applied. Figure 14.a shows v_{nN} when SVM is uses zero vectors. The induced shaft voltage v_{shaft} is shown in Figure 14.b. It can be noted that v_{shaft} has the same shape as v_{nN} having a peak value of approximately 5 volts. On the other hand, Fig. 15 shows v_{nN} when zero vectors are replaced by the rotating vectors. As it has been said previously, v_{nN} is approximately 42% lower when rotating vectors are used. Therefore, it is expected that there would be a similar reduction in v_{shaft}. Fig. 15.b shows this reduction. In this case, the peak value of v_{shaft} does not exceed 2 volts.

Finally, in order to corroborate that the new modulation technique does not increase EMI perturbations, a conducted EMI comparison has been carried out. Both the current flowing through the ground motor cable I_{CM} and the global current I_G has been measured.

This experiment was implemented using a voltage/frequency control at 20 Hz with $V_{AN,BN,CN} = 120$ V input voltage and the current has been measured using a high frequency current probe.

Figure 16 shows I_{CM} spectrum measurement in the whole range of conducted EMI. Both modulation techniques are shown and are overlaid for comparison. In Fig.16.a the A band is represented and shows that the new modulation does not increase the EMI level. Also, Fig.16.b shows the B band which reflects that both modulations have a similar behaviour.

The global current I_G which flows through to ground plane is shown in Fig.17. In Fig.17.a, it can be observe that the new modulation slightly reduces the low frequency harmonics in the A band. In B band no difference is noticeable, as shown in Fig.17.b.

CONCLUSION

This paper presents an in-depth study based on the modification of the DSSVM-switching pattern in order to reduce the CM perturbations and consequently increase the machine life time. Such modification consists of replacing the zero vectors by the rotating vectors, which always introduce zero CM voltage.

The study addressed in the paper confirms the expected reduction of the CM voltage amplitude as well as its time

derivative and hence stress on the insulation system of the motor is significantly reduced. The results also imply that, the quantity of the damage due to EDM produced in the bearings would be reduced and consequently the motor operational life increased. On the other hand, the number of commutations is unfortunately increased and for low modulation indexes a harmonic degradation is introduced. Also the power losses are increased by around 6% when rotating vectors are applied, which are directly related to the increase in the number of switching events.

The modulation will increase flux variation inside of the motor due to switch between active vector to rotating one. This variation may vary machine efficiency depending on the construction of the individual motor but it is not expected to change significantly and the behavior of electrical motor will not be affected. In comparison, DTC based control creates higher flux variation inside the electrical motor. However, it has been proven that this control strategy delivers a high performance to the load.

Finally, experimental time and frequency results have also been reported to support all the claims made in the paper together with conducted EMI measurements in order to show that the new modulation technique does not increase the EMI emissions.

This technique does increase the switching losses of the converter and the THD of the input and output of the converter. It does however significantly reduce the common mode voltage generated by the converter which will in turn increase the life of the motor. The decision as to whether the technique would be a valid option would depend on the particular drive application that it would be applied to. As with many things, it is a compromise. If bearing degradation is of particular importance, then this technique should be applied. A hybrid solution which uses standard SVM for some of the operational range of the drive and the modified SVM could be used for the critical operating points could be envisaged to achieve the desired balance between increased loss and bearing life. The input filter of the MC could also be modified to accommodate the increased filtering requirement in order to lower the THD if necessary.

REFERENCES

[1] D. A. Rendusara and P. N. Enjeti, "An improved inverter output filter configuration reduces common and differential modes dv/dt at the motor terminals in PWM drive systems," *Power Electronics, IEEE Transactions on,* vol. 13, pp. 1135-1143, 1998.
[2] D. Dahl, D. Sosnowski, D. Schlegel, R. J. Kerkman, and M. Pennings, "Gear up your bearings," *Industry Applications Magazine, IEEE,* vol. 14, pp. 45-53, 2008.
[3] D. Busse, J. Erdman, R. J. Kerkman, D. Schlegel, and G. Skibinski,

"Bearing currents and their relationship to PWM drives," *Power Electronics, IEEE Transactions on,* vol. 12, pp. 243-252, 1997.

[4] U. T. Shami and H. Akagi, "Identification and Discussion of the Origin of a Shaft End-to-End Voltage in an Inverter-Driven Motor," *Power Electronics, IEEE Transactions on,* vol. 25, pp. 1615-1625, 2010.

[5] U. T. Shami and H. Akagi, "Experimental Discussions on a Shaft End-to-End Voltage Appearing in an Inverter-Driven Motor," *Power Electronics, IEEE Transactions on,* vol. 24, pp. 1532-1540, 2009.

[6] J. Ollila, T. Hammar, J. Iisakkala, and H. Tuusa, "On the bearing currents in medium power variable speed AC drives," in *Electric Machines and Drives Conference Record, 1997. IEEE International*, 1997, pp. MD1/1.1-MD1/1.3.

[7] A. Muetze and A. Binder, "Calculation of Motor Capacitances for Prediction of the Voltage Across the Bearings in Machines of Inverter-Based Drive Systems," *Industry Applications, IEEE Transactions on,* vol. 43, pp. 665-672, 2007.

[8] A. Muetze and A. Binder, "Calculation of Circulating Bearing Currents in Machines of Inverter-Based Drive Systems," *Industrial Electronics, IEEE Transactions on,* vol. 54, pp. 932-938, 2007.

[9] R. F. Schiferl and M. J. Melfi, "Bearing current remediation options," *Industry Applications Magazine, IEEE,* vol. 10, pp. 40-50, 2004.

[10] C. Shaotang and T. A. Lipo, "Bearing currents and shaft voltages of an induction motor under hard- and soft-switching inverter excitation," *Industry Applications, IEEE Transactions on,* vol. 34, pp. 1042-1048, 1998.

[11] H. Akagi and S. Tamura, "A Passive EMI Filter for Eliminating Both Bearing Current and Ground Leakage Current From an Inverter-Driven Motor," *Power Electronics, IEEE Transactions on,* vol. 21, pp. 1459-1469, 2006.

[12] A. Muetze, V. Niskanen, and J. Ahola, "On radio-frequency based detection of high-frequency circulating bearing current flow," *Industry Applications, IEEE Transactions on,* vol. PP, pp. 1-1, 2014.

[13] A. Muetze and A. Binder, "Practical Rules for Assessment of Inverter-Induced Bearing Currents in Inverter-Fed AC Motors up to 500 kW," *Industrial Electronics, IEEE Transactions on,* vol. 54, pp. 1614-1622, 2007.

[14] A. Muetze and H. W. Oh, "Application of Static Charge Dissipation to Mitigate Electric Discharge Bearing Currents," *Industry Applications, IEEE Transactions on,* vol. 44, pp. 135-143, 2008.

[15] A. Binder and A. Muetze, "Scaling Effects of Inverter-Induced Bearing Currents in AC Machines," *Industry Applications, IEEE Transactions on,* vol. 44, pp. 769-776, 2008.

[16] A. L. Julian, G. Oriti, and T. A. Lipo, "Elimination of common-mode voltage in three-phase sinusoidal power converters," *Power Electronics, IEEE Transactions on,* vol. 14, pp. 982-989, 1999.

[17] S. Ogasawara, H. Ayano, and H. Akagi, "An active circuit for cancellation of common-mode voltage generated by a PWM inverter," *Power Electronics, IEEE Transactions on,* vol. 13, pp. 835-841, 1998.

[18] K. Kobravi, R. Iravani, and H. Kojori, "3-Leg/4-Leg Matrix Converters Generalized Modulation Strategy- Part II: Implementation and Verification," *Industrial Electronics, IEEE Transactions on,* vol. PP, pp. 1-1, 2012.

[19] J. Rodriguez, M. Rivera, J. W. Kolar, and P. W. Wheeler, "A Review of Control and Modulation Methods for Matrix Converters," *Industrial Electronics, IEEE Transactions on,* vol. 59, pp. 58-70, 2012.

[20] W. Xingwei, L. Hua, S. Hongwu, and F. Bo, "A Research on Space Vector Modulation Strategy for Matrix Converter Under Abnormal Input-Voltage Conditions," *Industrial Electronics, IEEE Transactions on,* vol. 59, pp. 93-104, 2012.

[21] A. Trentin, P. Zanchetta, J. Clare, and P. Wheeler, "Automated Optimal Design of Input Filters for Direct AC/AC Matrix Converters," *Industrial Electronics, IEEE Transactions on,* vol. 59, pp. 2811-2823, 2012.

[22] R. Cardenas, C. Juri, R. Pena, J. Clare, and P. Wheeler, "Analysis and Experimental Validation of Control Systems for Four-Leg Matrix Converter Applications," *Industrial Electronics, IEEE Transactions on,* vol. 59, pp. 141-153, 2012.

[23] C. Xia, J. Zhao, Y. Yan, and T. Shi, "A Novel Direct Torque Control of Matrix Converter-Fed PMSM Drives Using Duty Cycle Control for Torque Ripple Reduction," *Industrial Electronics, IEEE Transactions on,* vol. 61, pp. 2700-2713, 2014.

[24] L. Empringham, L. de Lillo, and M. Schulz, "Design Challenges in the use of Silicon Carbide JFETs in Matrix Converter Applications," *Power Electronics, IEEE Transactions on,* vol. PP, pp. 1-1, 2013.

[25] C. Han Ju and P. N. Enjeti, "An approach to reduce common-mode voltage in matrix converter," *Industry Applications, IEEE Transactions on,* vol. 39, pp. 1151-1159, 2003.

[26] L. Hong-Hee, H. M. Nguyen, and J. Eui-Heon, "A study on reduction of common-mode voltage in matrix converter with unity input power factor and sinusoidal input/output waveforms," in *Industrial Electronics Society, 2005. IECON 2005. 31st Annual Conference of IEEE*, 2005, p. 7 pp.

[27] C. Ortega, A. Arias, C. Caruana, and M. Apap, "Common mode voltage in DTC drives using matrix converters," in *Electronics, Circuits and Systems, 2008. ICECS 2008. 15th IEEE International Conference on*, 2008, pp. 738-741.

[28] R. Vargas, U. Ammann, J. Rodriguez, and J. Pontt, "Predictive Strategy to Control Common-Mode Voltage in Loads Fed by Matrix Converters," *Industrial Electronics, IEEE Transactions on,* vol. 55, pp. 4372-4380, 2008.

[29] R. K. Gupta, K. K. Mohapatra, A. Somani, and N. Mohan, "Direct-Matrix-Converter-Based Drive for a Three-Phase Open-End-Winding AC Machine With Advanced Features," *Industrial Electronics, IEEE Transactions on,* vol. 57, pp. 4032-4042, 2010.

[30] T. D. Nguyen and H. H. Lee, "A New SVM Method for an Indirect Matrix Converter With Common-Mode Voltage Reduction," *Industrial Informatics, IEEE Transactions on,* vol. 10, pp. 61-72, 2014.

[31] T. D. Nguyen and L. Hong-Hee, "Modulation Strategies to Reduce Common-Mode Voltage for Indirect Matrix Converters," *Industrial Electronics, IEEE Transactions on,* vol. 59, pp. 129-140, 2012.

[32] J. Espina, C. Ortega, A. Arias, and J. Balcells, "Space Vector Modulation strategy to reduce the Common Mode perturbations in Matrix Converters," *IEICE Electronics Express,* vol. 7, pp. 281-287, 2010.

[33] D. Casadei, G. Serra, A. Tani, and L. Zarri, "Matrix converter modulation strategies: a new general approach based on space-vector representation of the switch state," *Industrial Electronics, IEEE Transactions on,* vol. 49, pp. 370-381, 2002.

[34] J. F. Kolar, T. Krismer, F. Round, S., "The essence of three-phase AC/AC converter systems," *Przeglad Elektrotechniczny,* pp. 14-29, July 2008

[35] L. Empringham, J. W. Kolar, J. Rodriguez, P. W. Wheeler, and J. C. Clare, "Technological Issues and Industrial Application of Matrix Converters: A Review," *Industrial Electronics, IEEE Transactions on,* vol. 60, pp. 4260-4271, 2013.

[36] M. Rivera, A. Wilson, C. A. Rojas, J. Rodriguez, J. R. Espinoza, P. W. Wheeler*, et al.*, "A Comparative Assessment of Model Predictive Current Control and Space Vector Modulation in a Direct Matrix Converter," *Industrial Electronics, IEEE Transactions on,* vol. 60, pp. 578-588, 2013.

[37] T. F. Podlesak, D. C. Katsis, P. W. Wheeler, J. C. Clare, L. Empringham, and M. Bland, "A 150-kVA vector-controlled matrix converter induction motor drive," *Industry Applications, IEEE Transactions on,* vol. 41, pp. 841-847, 2005.

[38] M. Aten, C. Whitley, G. Towers, P. Wheeler, J. Clare, and K. Bradley, "Dynamic performance of a matrix converter driven electro-mechanical actuator for an aircraft rudder," in *Power Electronics, Machines and Drives, 2004. (PEMD 2004). Second International Conference on (Conf. Publ. No. 498)*, 2004, pp. 326-331 Vol.1.

[39] H. Hojabri, H. Mokhtari, and L. Chang, "Reactive Power Control of Permanent-Magnet Synchronous Wind Generator With Matrix Converter," *Power Delivery, IEEE Transactions on,* vol. PP, pp. 1-1, 2012.

[40] S. Zhang and K. J. Tseng, "Modeling, simulation and analysis of conducted common-mode EMI in matrix converters for wind turbine generators," in *Power Electronics and Motion Control Conference, 2008. EPE-PEMC 2008. 13th*, 2008, pp. 2516-2523.

[41] N. Holtsmark, H. J. Bahirat, M. Molinas, B. A. Mork, and H. K. Hoidalen, "An All-DC Offshore Wind Farm With Series-Connected Turbines: An Alternative to the Classical Parallel AC Model?," *Industrial Electronics, IEEE Transactions on,* vol. 60, pp. 2420-2428, 2013.

[42] S. Khwan-On, L. De Lillo, L. Empringham, and P. Wheeler, "Fault-Tolerant Matrix Converter Motor Drives With Fault Detection of Open Switch Faults," *Industrial Electronics, IEEE Transactions on,* vol. 59, pp. 257-268, 2012.

[43] N. Taib, B. Metidji, T. Rekioua, and B. Francois, "Novel Low-Cost Self-Powered Supply Solution of Bidirectional Switch Gate Driver for Matrix Converters," *Industrial Electronics, IEEE Transactions on,* vol. 59, pp. 211-219, 2012.

[44] P. W. Wheeler, J. Rodriguez, J. C. Clare, L. Empringham, and A.

Weinstein, "Matrix converters: a technology review," *Industrial Electronics, IEEE Transactions on,* vol. 49, pp. 276-288, 2002.

[45] J. K. Kang, T. Kume, H. Hara, and E. Yamamoto, "Common-mode voltage characteristics of matrix converter-driven AC machines," in *Industry Applications Conference, 2005. Fourtieth IAS Annual Meeting. Conference Record of the 2005*, 2005, pp. 2382-2387 Vol. 4.

[46] C. Ortega, A. Arias, C. Caruana, and M. Apap, "Reduction of the common mode voltage of a matrix converter fed direct torque control," *IEICE Electronics Express,* vol. 7, pp. 1044-1050, 2010.

Jordi Espina received the M. Eng and PhD degrees form the Universitat Politècnica de Catalunya (UPC), Catalonia, Spain, in 2005 and 2011 respectively..

He is currently a Research Fellow with Power Electronics Machines and Control group (PEMC), Nottingham university.

His research interests are variable-speed drive systems, EMC and power electronics converters

Carlos Ortega (M'10) received the B. Eng. degree in Electronics Engineering from the Escola Universitària Salesiana de Sarrià (EUSS), Barcelona, the M. Eng. and the PhD. degrees form the Universitat Politècnica de Catalunya (UPC), Catalonia, Spain, in 1998, 2003 and 2008 respectively.

From 1998 to 2001 he was with the Technology Transfer Department at EUSS. In 2002 he was appointed Lecturer in Electrical and Electronic Engineering at the same university.

In 2005 he joined the Power Electronics and control Department at the University of Malta as a researcher and part time lecturer.

He is currently collaborating with the Terrassa Industrial Electronics Group, Department of Electronics Engineering, UPC.

His current research interests include Power Electronics Converters and modulation strategies, high-performance AC Drives and Sensorless Control of electrical machines.

Dr. Ortega is a member of IEEE Industrial Electronics Society.

Liliana de Lillo (M'09) Received an M.Eng Degree in Electronic Engineering from Politecnico di Bari, Italy in 2001. She joined the Power Electronics, Machines and control group at the University of Nottingham and received a PhD degree in Electrical Engineering in 2006. She now works within the group as a Senior research fellow with interests in Direct AC-AC converters, Fault tolerant systems, More Electric Aircraft applications and AC Drives

Lee Empringham (M'10) Received a B.Eng (hons) degree in Electrical and Electronic Engineering from the University of Nottingham, UK in 1996. He then joined the Power Electronics, Machines and Control Group within the School of Electrical and Electronic Engineering at the University of Nottingham, UK to work on matrix converter commutation techniques. He received his PhD degree in November 2000.

Since then he has been employed by the group as a research fellow to support different ongoing matrix converter projects and has recently been appointed to the position of Principal research Fellow. His research interests include Direct AC-AC power conversion, Variable Speed AC Motor Drives using different circuit topologies and More-Electric / Electric Aircraft applications.

Dr Lee Empringham is a member of the Institution of Electrical Engineers and the Institute of Electrical and Electronic Engineers.

Josep Balcells (M'95-S'06) was born in Spain, in 1949. Received the Master and PhD degrees in Industrial Engineering from the Universitat Politècnica de Catalunya, Spain, in 1975 and 1983, respectively.

From 1978 to 1986, he was the head of R&D in AGUT SA (now a GE-group company). Since 1986 he is Professor at the Electronics Engineering Department of UPC, and technical consultant of CIRCUTOR GROUP.

His research interests include EMC in power systems, renewable energy systems, and design of power converters. He is author of several books and papers related with EMC in power systems, power quality measurement and filtering and has been responsible for several research projects funded by the Spanish Ministries of Science and Technology and Industry, and by the European Union.

Dr. Balcells is a Senior Member of IEEE and is serving as an Associate Editor of the IEEE TRANSACTIONS ON INDUSTRIAL ELECTRONICS since 2004.

Antoni Arias (M'03) received the BEng degree in electrical engineering, MEng and PhD degrees in control and electronic engineering from the Universitat Politècnica de Catalunya, Catalonia, Spain, in 1993, 1997 and 2001 respectively.

Since 1996 he has been a Lecturer at the Universitat Politècnica de Catalunya and was appointed as an Associate Professor in 2002 at the same University.

In 1999 he was a visiting research assistant and part time lecturer at the University of Glamorgan, UK. In 2003 and 2004 he joined as a Visiting Fellow the Power Electronics, Machines and Control Group at the University of Nottingham, UK.

His research interests are variable-speed drive systems, power electronics converters and control strategies.